FOREX Publication
Open Access | Rapid and quality publishing

International Journal of Electrical and Electronics Research (IJEER)
Research Article | Volume 13, Issue 4 | Pages 886-899 | e-ISSN: 2347-470X

Performance Analysis of High Torque Density in Switched Reluctance Motor for Electric Transportation

Boyanasetti Venkata Sai Thrinath[1*], and Dr. Edwin Vijay Kumar Dokiburra[2]

[1]Research Scholar, Andhra University Trans-Disciplinary Research Hub, Department of Electrical Engineering, Andhra University, Visakhapatnam, India; Email: connectbvst@gmail.com
[2]Professor, Department of Electrical Engineering, Gayatri Vidya Parishad College of Engineering (Autonomous), Visakhapatnam, India; Email: edwin@gvpce.ac.in

***Correspondence:** *Boyanasetti Venkata Sai Thrinath; Email: connectbvst@gmail.com; Ph.: +91-6304706409*

ABSTRACT- In this paper, the detailed comparative study of high torque density switched reluctance motor (SRM) used in the electric transport is provided. By means of sophisticated simulation packages Motor Solve and Magnet Solve. The delivered outputs of the study models of SRM that have 3KW rating of output power, 2700 RPM rates of speed,10A rated currents and a rated torque of 10 Nm. Torque density, efficiency, and power to weight ratio are essential performance parameters that are comprehensively explored in simulation approaches. The comparison between the SRM structural design is established on the basis of performance in the challenging transportation applications. Results of simulation analysis also provide by choosing motor architectures to use on electric mobility platforms where size, efficiency and thermal concerns are essential. This paper discusses engineering insights and presents a viable engineering decision making design and implementation of the proposed electric motor technology in next generation transportation systems via the power of precise simulation driven evaluation.

Keywords: Switched Reluctance Motor (SRM), Torque Ripple Reduction, Electric Transportation, Torque Density, Finite Element Analysis (FEA).

ARTICLE INFORMATION

Author(s): Boyanasetti Venkata Sai Thrinath, Dr. Edwin Vijay Kumar Dokiburra;

Received: 05/07/2025; **Accepted:** 07/12/2025; **Published:** 30/12/2025;
E- ISSN: 2347-470X;
Paper Id: IJEER 0507-04;
Citation: 10.37391/ijeer.130429
Webpage-link:
https://ijeer.forexjournal.co.in/archive/volume-13/ijeer-130429.html

Publisher's Note: FOREX Publication stays neutral with regard to jurisdictional claims in Published maps and institutional affiliations.

1. INTRODUCTION

In [1] a technique has been investigated where in the current waveforms are shaped by the way of reducing the torque ripple and the noise in Switched Reluctance motors (SRMs). The method changes the current patterns of the motor to generate less vibrations and smooth torque. Their simulation and experimental evidence support their work and indicates that better motor operation is achieved without changing the hardware of the motor.

In [2] helps to cover the review of the strategy of torque ripples minimisation in Switched Reluctance Motors (SRMs) that is Indirect Torque Control (ITC) and Direct Torque Control (DTC). The authors examine the effects on the performance of an electric vehicle (EV) of the torque ripple and question the efficiency of ITC and DTC in reducing the unfortunate oscillations.

In [3] derived an online torque sharing technique (TSF) of SRMs as an effort to minimize torque ripple as well as copper losses. Their real time strategy when adapted to the conditions of operation work the efficiency is enhanced and changes in torque modes. In [4] proposed a self-regulating torque reference system used in TSF control of SRMs. Such a digital method enhances the consistency of the torque since it accommodates the variations in load requirements. The technique improves dynamics and minimizes torque ripple and is applicable in high-performance applications where high control demands are needed.

In [5] examined a new 12/8 segmental rotor SRM using permanent magnet assistance. This combined construction increases the torque density and improves the ripple using optimum magnetic flux paths. Better motor performance is reflected by finite element analysis and testing, which makes the design a promising candidate to high performance drives.

In [6] a designing of 6/4 SRM to solar powered water pumping systems with an agenda of improving the torque and eliminating the ripple content. They have maximized the geometry and the control of the motor in a way that makes it manage the variable solar input effectively. In [7] new power converter design was presented to minimize torque ripple in SRMs. Through the

FOREX Publication
Open Access | Rapid and quality publishing
International Journal of Electrical and Electronics Research (IJEER)
Research Article | Volume 13, Issue 4 | Pages 886-899 | e-ISSN: 2347-470X

achieved ability to control phase current, the converter reduces electromagnetic wobbles. With experimental validation, they demonstrate enhanced smoothness of torque, which is a compact and efficient solution to electric vehicles and any other high-demand motor system.

In [8] the influence of stator pole tip shapes on torque ripple in SRMs was examined. Through studying different geometrics, they were able to discover shapes which gave better flux distribution and ripple reduction. Their findings offer a structural way to improve SRM torque quality devoid of changing electrical control methods. In [9] three-dimensional gap structures of SRMs were used to enhance the static torque properties. They are designed to alter flux paths in the magnets minimizing torque ripple and maximizing average torque delivery.

In [10] torque and current ripple were studied in SynRMs based and WR-SMs-based integrated DC-DC converters. They do not specify anything SRM-specific, but their results reveal some consequences of the converter design on the torque smoothness. This tobacco focuses of the need of integrated electrical and machine design to achieve best ripple control of electric drive.

In [11] compare several topologies of converter to determine their influence on torque ripple in Switched Reluctance Motors (SRMs). Their scheme shows the effect of various converter topologies on torque smoothness, efficiency, switching losses. In [12] proposes the use of hybrid-excited SRM, devoid of permanent magnets, targeting the applications in electrical vehicles. The motor design represents high torque density that avoids the use of rare earth materials that would consume more materials and hence increase costs.

In [13] Optimization of rotor geometry attention has been focused to the optimization of rotor geometry to reduce torque ripple in SRMs. They are testing different rotors by finite element method (FEM) simulation to increase the uniformity of torque and decrease electromagnetic disturbances. The results of their work stress the significance of mechanical design improvements in providing quieter motor running, which is in the main in the fields of robotics and electric cars where precise and reliable control of the torque is needed.

In [14] investigated hybrid structures of non-permanent magnet excited Switched Reluctance Motors (SRMs) for the purpose of increasing the amount of available torque and lowering the use of the rare-earth materials. Their designs strike the balance between performance and cost relation by optimizing the magnetic structures with the aim of achieving better torque density and reducing ripple.

In [15] focus the torque ripple minimization of different SRM topologies on electromechanical brake systems based on finite element method (FEM) data. The result of their study is the analysis of how variations of configuration influence torque smoothness and braking power. The findings prove that certain topology optimizations have the capability to heavily reduce torque ripple, increasing safety and control in braking designs.

2. EXISTING TOPOLOGY

Switched Reluctance Motors (SRMs) are peculiar electric machines characterized by a fairly simple, robust construction. They work with the principle of reluctance torque at which rotor is attracted towards the least magnetic reluctance position. The stator and rotor both have salient poles and the current is switched electronically to stator windings to give continuous rotation with high efficiency and fault tolerance. As shown in *figure 1* SRM could be classified.

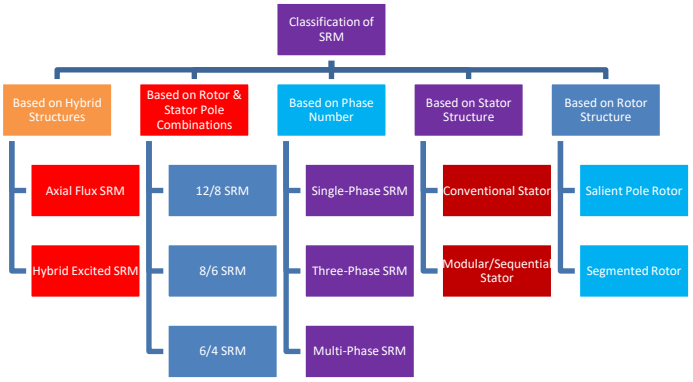

Figure 1. Classification of Switched Reluctance Motor (SRM)

(A) Classification Based on Rotor Structure

Switched Reluctance Motors are also characterized by Salient pole Rotor. Its prototype design which is characterized by protruding poles is fundamental in the creation of reluctance torque. These poles on the rotor are strongly attracted by the magnetic field on the stator and all of them orient themselves so the reluctance in the magnetic path is minimized. This intrinsic magnetic asymmetry in salient pole rotor forms the basis of SRM operation principle and makes its operation robust and ensures efficient production of torque.

(B) Classification Based on Stator Pole Structure

The design of the stator is important in the Salient Pole SRM. This is in form of big poles carrying concentrated windings, which directly generates the magnetic fields that pull the rotor. It is an easy construction and the design strengthens the magnetic power. Non-Salient Pole Stator may imply the use of distributed windings, but is not more common with SRMs. The 2-Phase or 3-Phase entries here has more to do with the number of sets of windings and electrical control and sets the number of phases of operation of the motor.

(C) Classification Based on Number of Poles

In this presence of pole configuration (Ns/Nr) and pole pairing critically determine the behavior of the SRM. 4/2 pole designs are less popular because they have large torque ripple and possible problems in operation. The 6/4 Pole design is a widespread three-phase standard and at that provides a reasonable tradeoff between performance and simplicity of

FOREX Publication
Open Access | Rapid and quality publishing
International Journal of Electrical and Electronics Research (IJEER)
Research Article | Volume 13, Issue 4 | Pages 886-899 | e-ISSN: 2347-470X

control. More poles or phases such as 8/6 and 12/8 smooth out torque and decrease the extent of ripple and enhance levels of fault tolerance, but at the cost of more complex power electronics and motor cost.

3. PROPOSED METHODOLOGY

(A) Classification Of Flux Barriers

By the method of controlling magnetic flux, rotor designs are categorized. The *figure 2(a)* includes the clarifications among conventional rotors that do not internalize any modifications and the flux-modulated rotors. The latter tactically use internal air gaps which are called as flux barriers to direct or deflect magnetic flow. These are either circumferential or radial barriers which are designed so as to improve the performance of the motor due to improved motor paths of magnetic reluctance within the rotor system.

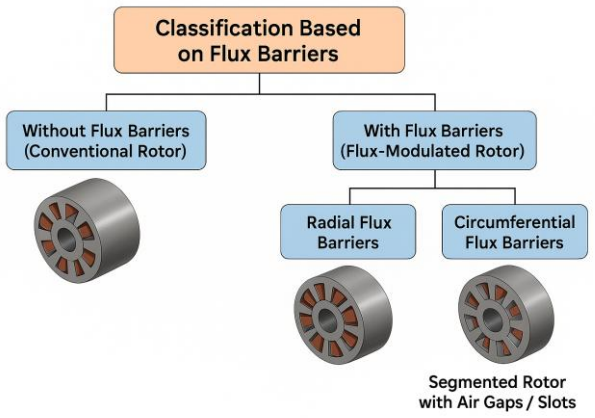

Figure 2(a). Classification based of flux barrier Layers of SRM

Rotors without flux barriers use a solid or laminated steel core where magnetic flux naturally follows the existing material path. This is the conventional design used in most electric motors, including standard SRMs. Since there are no internal obstacles, the magnetic flux flows directly through the rotor poles, resulting in a straightforward but less optimized magnetic circuit.

Rotors with flux barriers incorporate purposely placed air gaps or Nonmagnetic inserts to control how magnetic flux moves inside the rotor. Radial barriers block radial flux and redirect it along circumferential paths, while circumferential barriers interrupt flux flowing around the rotor. By altering flux patterns, these designs help improve torque density, reduce torque ripple and enhance overall motor performance.

(B) B–H Curve of M-19 29Ga Electrical Steel

The *figure 2(b)* represents the B H curve of M- 19 29Ga non-oriented electrical steel at 20^0C, and it is commonly used in SRM stator and rotor cores. When the magnetic field intensity (H) is low the curve rises steeply in flux density (B) so that there are high initial permeability and a good magnetization. As H increases, the curve gradually flattens, demonstrating a reduction in permeability as the steel approaches the saturation region. The flux density reaches approximately 2.2–2.4 T, after which further increase in H results in minimal improvement in B. This saturation characteristic emphasizes the need to limit peak flux levels in the motor design to prevent excessive core losses, heating and reduced torque performance. Due to its good compromise between permeability and saturation strength, M-19 29Ga is well-suited for high-performance SRM applications.

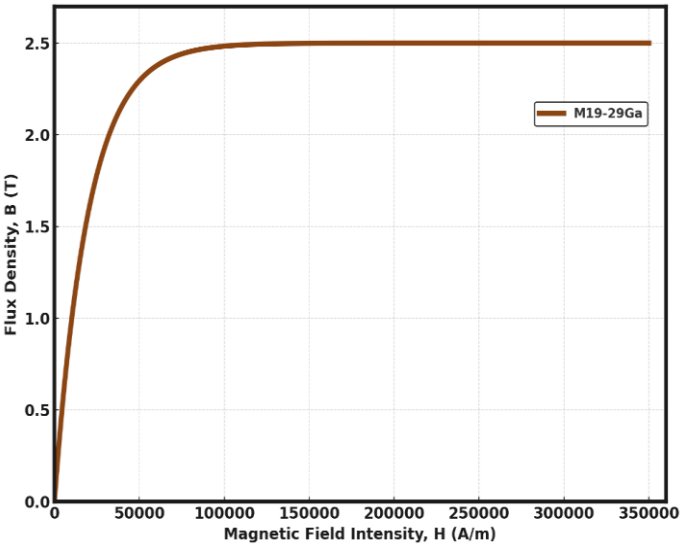

Figure 2(b). B-H curve of M19-29Ga

3.1. Mathematical Modelling for Designing of Switched Reluctance Motor

In the Finite Element Analysis (FEA) of a Switched Reluctance Motor (SRM) a number of fundamental assumptions are normally applied. They are that magnetic hysteresis was ignored, no time-harmonic influences are taken and the motor in not surrounded by external magnetic fields. Moreover, it is also assumed that the flux density of the magnetic field is not vary throughout the magnet length.

The Voltage equation is written as

$$\vartheta_k(t) = R_k * i_k(t) + \frac{d\lambda_k(\theta, i_k)}{dt} \quad (1)$$

Where,

$$\frac{d\lambda}{dt} = \frac{\partial\lambda}{\partial i} * \bar{i} + \frac{\partial\lambda}{\partial\theta} \cdot \bar{\theta} = L(\theta, i) * \bar{i} + i\frac{\partial L(\theta,i)}{\partial\theta} * \bar{\theta} \quad (2)$$

by substituting *equation (2)* in *(1)*

$$v_k = R_{k^*} i_k + L(\theta, i) * \bar{i}_k + i_k \omega \frac{\partial L(\theta,i)}{\partial\theta} \quad (3)$$

Flux Linkages $\lambda(\theta, i)$ is written in reluctance as

$$\lambda(\theta, i) = N * \emptyset(\theta, i) = \frac{N^2 * i}{R_m(\theta,i)} \quad (4)$$

$$L(\theta, i) = \frac{\partial\lambda}{\partial i} = \frac{N^2}{R_m(\theta,i)} \quad (5)$$

FOREX Publication
Open Access | Rapid and quality publishing
International Journal of Electrical and Electronics Research (IJEER)
Research Article | Volume 13, Issue 4 | Pages 886-899 | e-ISSN: 2347-470X

Where R_m is magnetic reluctance stated as

$$R_m = \frac{l}{\mu_0 \mu_\gamma A} \quad (6)$$

Single-layer flux barrier is usually a radial region of low magnetic cross section (slot/opening) inside the rotor pole that forces flux to take longer paths and concentrates flux into the pole tip.

Therefore, flux barrier depth in radial is written as

$$h_b = R_0 - R_{b,inner} \quad (7)$$

where $R_{b,inner}$ is the inner radius of the barrier region.
Air gap Reluctance is stated as

$$R_g = \frac{g}{\mu_0 A_g} \quad (8)$$

Reluctance due to flux barrier is written as

$$R_b = \frac{l_b}{\mu_0 A_b} \quad (9)$$

Where,

l_b= detour length & A_b= slot cross section area Reluctance due to core is written as

$$R_c = \frac{l_c}{\mu_0 \mu_r A_c} \quad (10)$$

Therefore, total magnetic reluctance is written as

$$R_m(\theta) = R_g(\theta) + R_b(\theta) + R_c(\theta) \quad (11)$$

The torque of the SRM is obtained by using magnetic co-energy which is written as

$$W_{co}(\theta, i) = \int_0^i \lambda(\theta, i')\, di' = \frac{1}{2} L(\theta) i^2 \quad (12)$$

Therefore, electric torque due to co-energy is

$$T_e(\theta, i) = \frac{\partial w_{CO}(\theta, i)}{\partial \theta}\Big|_i \quad (13)$$

If L is independent of 'i' then linear toque is

$$T_e(\theta, i) = \frac{1}{2} i^2 \frac{\partial L(\theta)}{\partial \theta} \quad (14)$$

Copper loss of SRM is stated by

$$P_{cu} = I^2{}_{rms} * R \quad (15)$$

Hysteresis losses due to core are given by

$$P_h = K_h f^a B_{max}^b \quad (16)$$

Mechanical losses are stated by

$$P_{mech} = B\omega^2 + P_{\omega indage} \quad (17)$$

Peak torque per pole when in alignment range is stated by

$$T_{max} = \frac{1}{2} * i^2 * N^2 * \frac{\Delta R}{R^2{}_{min}} * \frac{1}{\Delta\theta} \quad (18)$$

Equivalently torque due to reluctance is

$$T_e(\theta, i) = -\frac{1}{2} i^2 N^2 \frac{R_m{}'(\theta)}{R_m(\theta)^2} \quad (19)$$

Instantaneous power for power balance between electrical and mechanical domain of SRM is

$$P_{elec} = v * i = Ri^2 + i\frac{d\lambda}{dt} \quad (20)$$

Finally Mechanical power is stated as

$$P_{mech} = T_e * \omega = i\omega \frac{\partial \lambda}{\partial \theta} \quad (21)$$

The cogging Torque of SRM is expressed as

$$T_{cogg} = -\frac{1}{2} \phi^2 \frac{dR}{d\theta} \quad (22)$$

The speed, average toque and torque ripples are expressed as

$$N = \frac{P*60}{2*\pi*T} \quad (23)$$

Output Power is determined by

$$P = \frac{2*\pi*N*T}{60} \quad (24)$$

Average Torque is calculated by using formula

$$T_{avg} = \frac{T_{max} + T_{min}}{2} \quad (25)$$

Torque Ripple is calculated by

$$T_{ripple} = \frac{T_{max} - T_{min}}{T_{avg}} \quad (26)$$

Specific Torque Density is determined by

$$\text{Specific Torque} = \frac{T}{m} \quad (27)$$

Where m = Machine mass in Kg

3.2. Finite Element Analysis of Switched Reluctance Motor of Existing and Proposed Structural Designs

3.2.1. Three phase 6 Stator pole & 2 rotor poles of exiting SRM

Switched Reluctance Motors (SRMs) are electromagnetic machines that generate torque through the principle of variable reluctance. Unlike traditional motors, SRMs have a simple

FOREX Publication
Open Access | Rapid and quality publishing
International Journal of Electrical and Electronics Research (IJEER)
Research Article | Volume 13, Issue 4 | Pages 886-899 | e-ISSN: 2347-470X

design with salient poles on both stator and rotor and they lack permanent magnets or windings on the rotor. This contributes to high reliability and cost-effectiveness, especially in harsh environments.

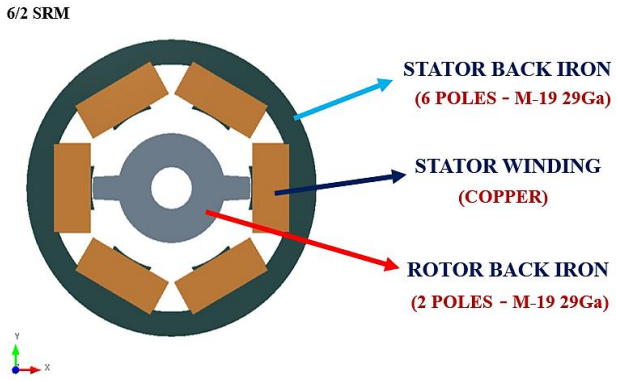

Figure 3(a). Structural design of 6/2 base SRM

Figure 3(a) is a 6/2 switched reluctance motor (SRM), featuring six stator poles and four rotor poles. It operates by sequentially energizing phase windings to create magnetic attraction between stator and rotor poles. The rotor moves to minimize reluctance, enabling rotation. Its simple structure ensures robustness and fault tolerance.

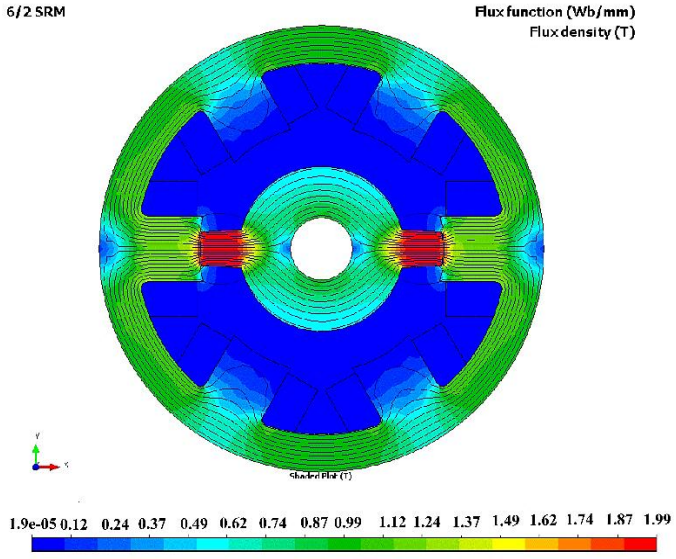

Figure 3(b). Flux distribution of 6/2 base SRM at 1.99T

The *figure 3(b)* is a 6/2 switched reluctance motor (SRM) shown illustrates magnetic flux distribution during phase excitation. Magnetic flux flows from stator poles to rotor poles, following the path of least reluctance. The flux density reaches a peak of approximately 1.99 Tesla near the aligned stator poles.

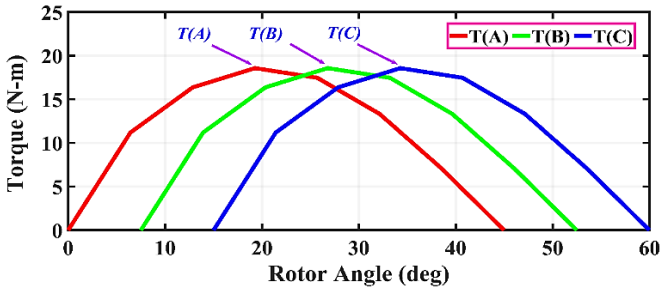

Figure 3(c). Torque characteristics of existing 3 phase 6/2 base SRM

3.2.2. Three phase 6 Stator pole & 2 rotor poles of Proposed SRM

The proposed 6/2 switched reluctance motor shown in *figure 4(a)* incorporates a six-pole stator equipped with copper windings and supported by an M-19 laminated steel back iron to ensure strong magnetic coupling. The two-pole rotor, also constructed from M-19 steel integrates carefully positioned flux barriers designed to direct and regulate the magnetic flux within the rotor structure. This configuration enhances flux control, improves torque production, and contributes to reduced torque ripple, resulting in a more efficient and refined electromagnetic performance suitable for advanced motor applications.

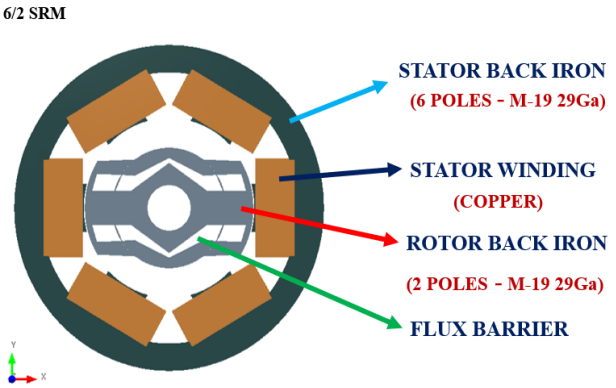

Figure 4(a). Structural design of proposed 6/2 SRM

Both stator and rotor cores are designed using M19-29Ga electrical steel, enabling accurate representation of nonlinear magnetic behavior with reduced iron losses. The internal flux-barrier region is treated as a nonmagnetic domain to enforce flux guidance and enhance saliency characteristics. Phase windings are driven with time-varying current excitation sequences replicating practical SRM drive operation. An infinite boundary is introduced at the outer air domain to prevent artificial flux confinement. Electromagnetic performance including torque, co-energy and flux linkage is evaluated using a transient magnetic solver across multiple rotor positions.

FOREX Publication
Open Access | Rapid and quality publishing
International Journal of Electrical and Electronics Research (IJEER)
Research Article | Volume 13, Issue 4 | Pages 886-899 | e-ISSN: 2347-470X

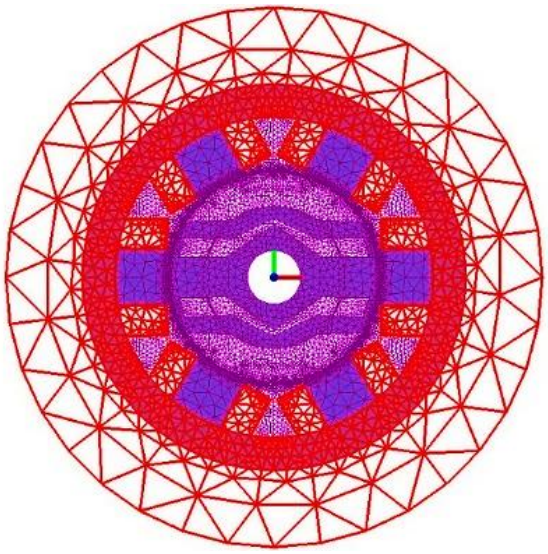

Figure 4(b). 2D Meshing design of proposed 6/2 SRM

The proposed 6/2 switched reluctance motor (SRM) in *figure 4(b)* configuration in 2D presented in this study at boundary condition of 1mm incorporates a single layer flux barrier within the rotor to increase the magnetic reluctance difference between aligned and unaligned positions, thereby improving torque output. A finer triangular mesh is used in the air gap, stator tooth and rotor pole regions to accurately capture magnetic field variations The complete motor geometry is discretized using an adaptive finite element mesh to achieve high accuracy in electromagnetic field evaluation while minimizing computational burden. In this 6/2 SRM is initialized with 2D mesh and the maximum element size is given a 1mm to get the hysteresis, eddy current, copper and total losses of 9.583W, 0.469W,660W and 670.052W respectively.

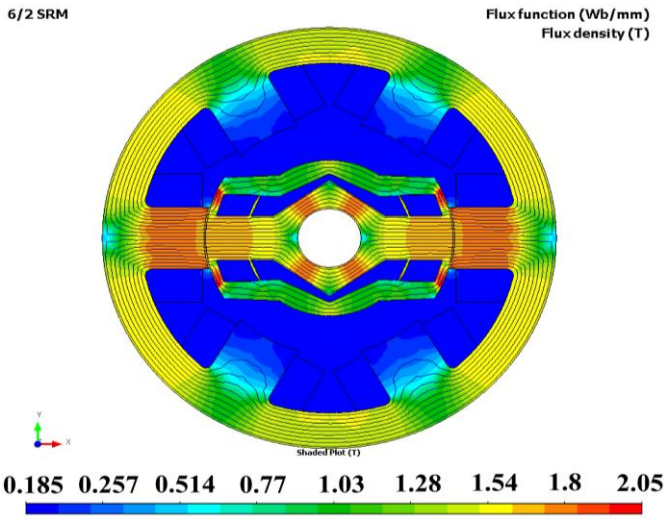

Figure 4(c). Flux distribution of proposed 6/2 SRM at 2.05T

The *figure 4(c)* infers the simulated flux distribution of the proposed 6/2 single layered flux barrier Switched reluctance motor illustrates a well-defined magnetic path concentrated across the aligned stator and rotor poles. The field lines indicate strong flux interaction through the rotor core, with the flux barriers effectively redirecting the magnetic field to reduce leakage and enhance the usable flux in the active region having a flux density of 2.05 tesla.

The flux density plot of the 6/2 SRM shows that the magnetic flux is primarily concentrated along the stator tooth tips and the rotor saliencies during phase excitation. High flux density regions near the air gap and rotor poles indicate strong magnetic coupling and active torque generation. The single layer flux barrier effectively directs the flux through the intended magnetic path while reducing leakage in non-active regions.

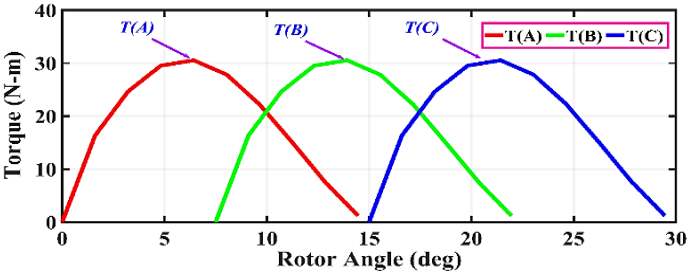

Figure 4(d). Torque characteristics of proposed 3 phase 6/2 SRM

The *figure 4(d)* infers the torque waveform produced by the Switched reluctance Motor of 6 stator poles and 2 rotor poles having the toque vales of maximum, minimum, average, Specific Torque density and Power Density are 30.5 N.m, 20.9 N.m and 25.7 N.m,12.12 N.m/Kg and 1415.09W/Kg with torque ripple as 0.37.

3.2.3. Three phase 6 Stator pole & 4 rotor poles of existing SRM

The 6/4 switched reluctance motor consists of six salient stator poles and four rotor poles, arranged to provide continuous electromagnetic torque during phase commutation. The stator is constructed using M19-29Ga electrical steel, offering high magnetic permeability and reduced core loss, while the copper windings are concentrically placed around each stator pole for efficient excitation.

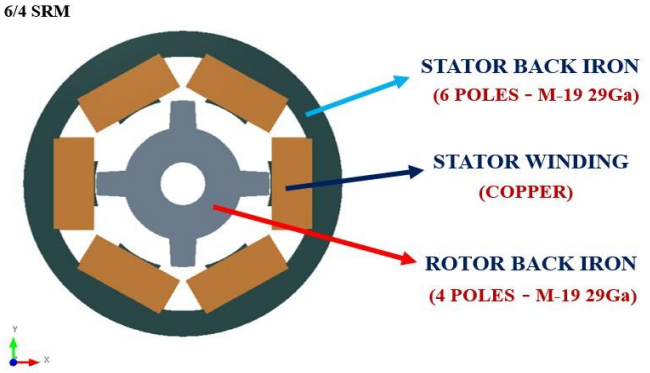

Figure 5(a). Structural design of 6/4 SRM

The rotor also formed with M19-29Ga steel, contains four salient poles designed to guide the magnetic flux during energization and support reluctance torque production. The mechanical

FOREX Publication
Open Access | Rapid and quality publishing
International Journal of Electrical and Electronics Research (IJEER)
Research Article | Volume 13, Issue 4 | Pages 886-899 | e-ISSN: 2347-470X

structure ensures strong magnetic saliency and provides adequate space for rotor movement while maintaining a uniform air-gap around the circumference.

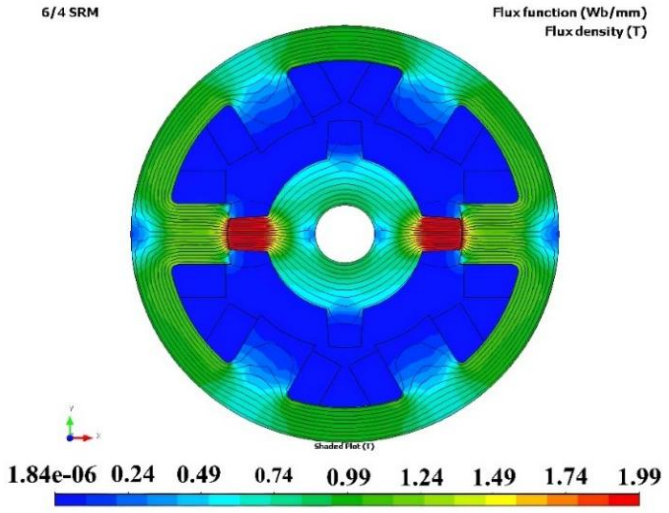

Figure 5(b). Flux distribution of 6/4 SRM at 1.99T

The magnetic flux density distribution in *figure 5(b)* of the 6/4 switched reluctance motor under an excited phase condition demonstrates efficient flux linkage between the aligned stator and rotor poles. The smooth and symmetric flux pattern reflects controlled magnetic guidance with limited leakage into inactive poles, highlighting the effectiveness of the motor geometry in maintaining uniform magnetic performance. Magnetic flux flows through the excited stator poles toward aligned rotor poles with the flux density peaks around 1.99 T.

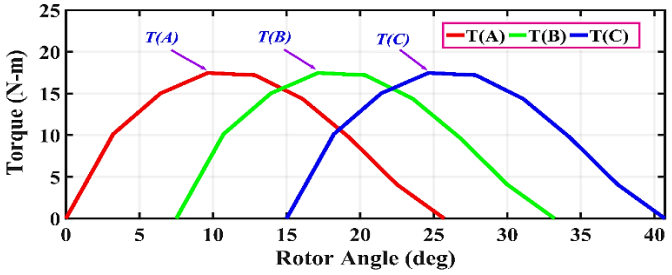

Figure 5(c). Torque characteristics of 3 phase 6/4 base SRM

The *figure 5(c)* infers the torque waveform produced by the Switched reluctance Motor of 6 stator poles and 4 rotor poles having the toque vales of maximum, minimum, average, Specific Torque density and Power Density are 17.5 Nm, 15.6 Nm, 16.55 Nm, 7.25 Nm/Kg, and 1315.78W/Kg with torque ripple as 0.114 Nm.

3.2.4. Three phase 6 Stator pole & 4 rotor poles of Proposed SRM

The single layer flux barrier in the 6/4 SRM rotor increases the difference in magnetic reluctance between aligned and unaligned positions, which directly enhances torque production based on the reluctance torque principle. The barrier restricts flux penetration through the low saliency side of the rotor pole and forces the magnetic field to follow a more concentrated path during phase excitation. This controlled flux guidance reduces leakage flux, improves magnetic coupling in the active poles and leads to stronger alignment forces.

As a result, both the peak torque and the average torque are improved, while the distribution of flux across the rotor becomes more uniform, contributing to lower magnetic saturation and reduced torque ripple.

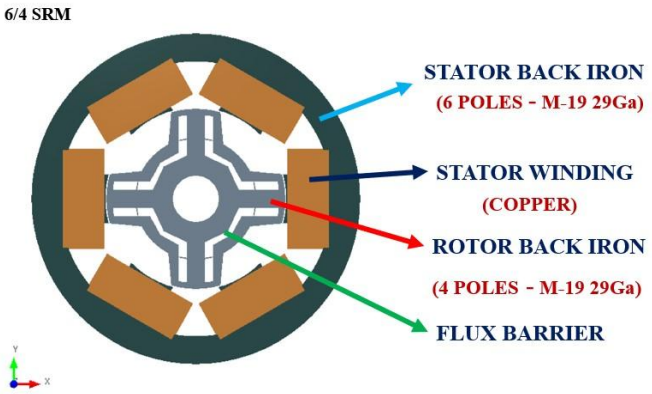

Figure 6(a). Structural design of proposed 6/4 SRM

The *figure 6(a)* infers 6/4 SRM model with a single layer flux barrier is discretized using a non-uniform triangular finite element mesh. A high mesh density is enforced in the air-gap region, at the stator tooth tips, around the rotor poles and along the flux-barrier interfaces to resolve steep flux gradients and local saturation. The stator and rotor back irons are meshed with moderate element size, while the outer surrounding air region is modelled with a gradually coarser mesh to limit the total element count and reduce computational time without compromising field accuracy.

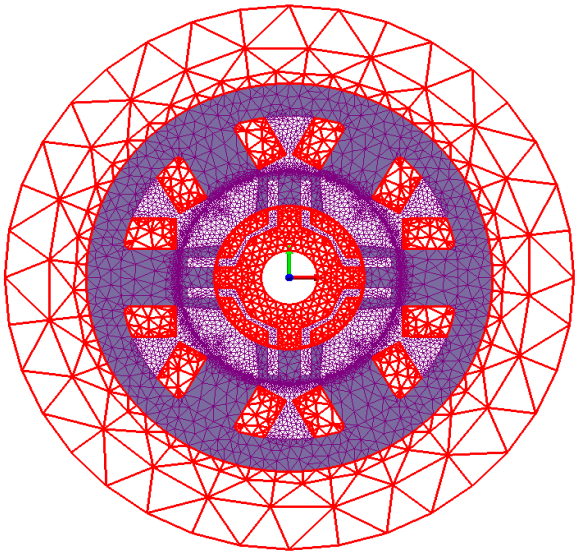

Figure 6(b). 2D Meshing design of proposed 6/4 SRM

FOREX Publication
Open Access | Rapid and quality publishing
International Journal of Electrical and Electronics Research (IJEER)
Research Article | Volume 13, Issue 4 | Pages 886-899 | e-ISSN: 2347-470X

This *figure 6(b)* is 2D mesh at boundary condition of 1mm represents a 6/4 SRM with a single layer flux barrier. A finer triangular mesh is used in the air-gap, stator tooth and rotor pole regions to accurately capture magnetic field variations. The flux barrier area is also refined to evaluate its influence on flux guidance. Coarser elements are applied toward the outer stator domain to reduce computation while maintaining solution accuracy. Overall, the mesh focuses detail where electromagnetic gradients are highest for reliable torque and flux. In this 6/4 SRM is initialized with 2D mesh and the maximum element size is given a 1mm to get the hysteresis, eddy current, copper and total losses of 17.07W, 0.969W, 289.440W and 307.426W respectively.

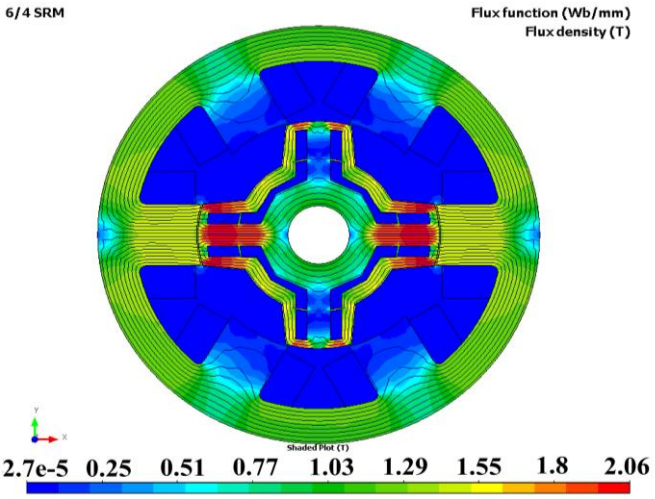

Figure 6(c). Flux distribution of proposed 6/4 SRM at 2.06T

The *figure 6(c)* displays the magnetic flux distribution in a 6/4 SRM under excitation. The flux lines travel from the energized stator poles through the rotor poles and return *via* the stator back-iron, forming a closed magnetic circuit. Higher flux density is observed in the air-gap and aligned rotor-stator poles, where values approach saturation levels around 2.06 T. The visualization confirms correct flux guidance through the active poles and efficient utilization of the magnetic core.

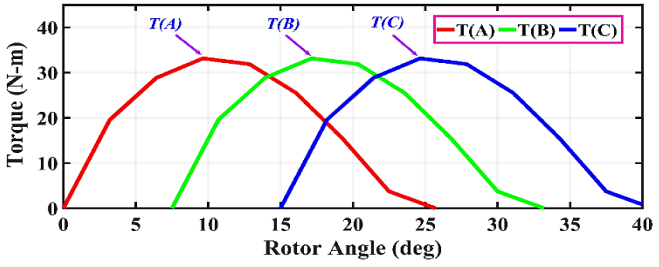

Figure 6(d). Torque characteristics of proposed 3 phase 6/4 SRM

The *figure 6(d)* infers the torque waveform produced by the Switched reluctance Motor of 6 stator poles and 4 rotor poles having the toque vales of maximum, minimum, average, specific torque density and power density are 33.1 Nm, 29.3 Nm, 31.2 N.m,14.24 Nm/Kg and1369.86 W/Kg with torque ripple as 0.121.

3.2.5. Three phase 12 Stator pole & 8 rotor poles of existing SRM

The *figure 7(a)* presents a cross-sectional view of a 12/8 Switched Reluctance Motor (SRM), consisting of twelve wound stator poles and eight unwound rotor poles. The stator and rotor cores are fabricated using laminated M-19 electrical steel to reduce magnetic losses and provide an efficient flux path. Copper windings are placed on the stator poles and torque is produced through the variation of magnetic reluctance as rotor poles move toward aligned positions during phase excitation. This configuration highlights the simplicity, robustness and flux-focused structure that characterize SRM technology.

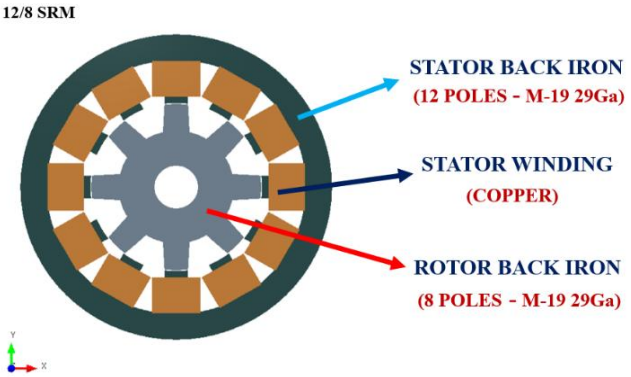

Figure 7(a). Structural design of 12/8 base SRM

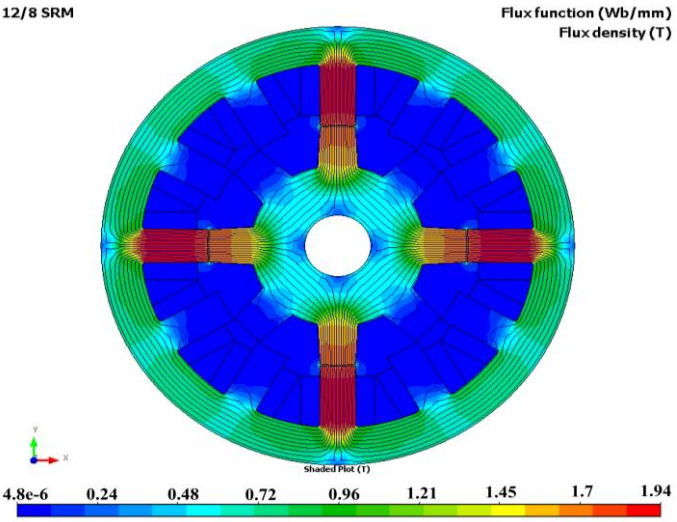

Figure 7(b). Flux distribution of 12/8 base SRM at 1.94T

The *figure7(b)* is flux density shows how magnetic flux travels inside the 12/8 base SRM when one phase is energized. The energized stator poles attract the nearest rotor poles, causing high magnetic flux in that region. This strong flux alignment generates torque that pulls the rotor toward the aligned position. The areas in blue show low flux because those stator poles are not currently energized. As each phase is excited in sequence, the flux path shifts and the rotor continue to rotate. Magnetic flux flows through the excited stator poles toward aligned rotor poles with the flux density peaks around 1.94 T.

FOREX Publication
Open Access | Rapid and quality publishing
International Journal of Electrical and Electronics Research (IJEER)
Research Article | Volume 13, Issue 4 | Pages 886-899 | e-ISSN: 2347-470X

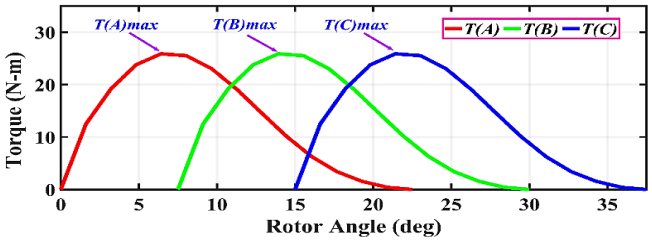

Figure 7(c). Torque characteristics of 3 phase 12/8 Base SRM

The *figure 7(c)* infers the torque waveform produced by the Switched reluctance Motor of 12 stator poles and 8 rotor poles having the toque vales of maximum, minimum, average, Specific Torque density and Power Density are 25.9 Nm, 19.8 Nm, 22.85 Nm, 8.13N.m/Kg and 1067.61W/Kg with torque ripple as 0.266.

3.2.6. Three phase 12 Stator pole & 8 rotor poles of Proposed SRM

This *figure 8(a)* shows the cross-section of a 12/8 Switched Reluctance Motor that includes a single-layer flux barrier structure. The stator contains 12 salient poles with copper windings, which create magnetic excitation when energized. The rotor has 8 poles made of laminated steel without any windings or magnets. Flux barriers are introduced within the rotor to control the magnetic flux path, reduce unwanted flux leakage and improve torque characteristics. The stator and rotor back irons provide a strong magnetic path and structural support for the motor. When current flows through a stator phase, the magnetic flux travels through the rotor toward the aligned position, producing torque for rotation.

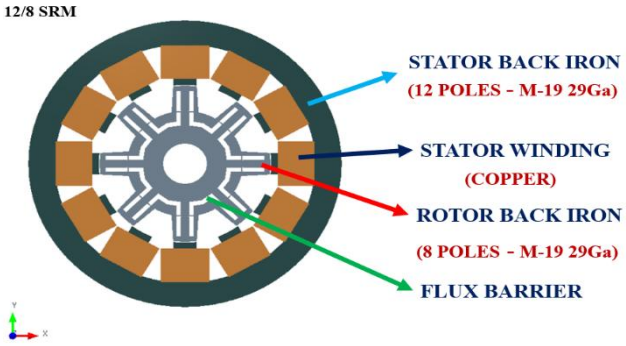

Figure 8(a). Structural design of proposed 12/8 SRM

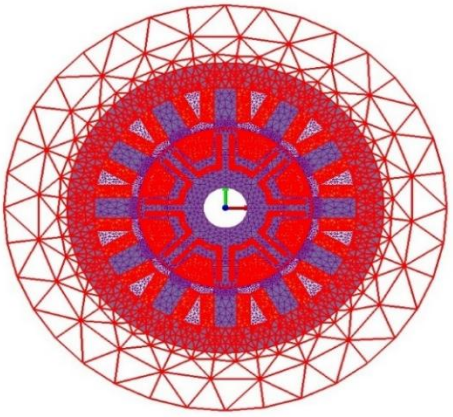

Figure 8(b). 2D Meshing design of proposed 12/8 SRM

This *figure 8(b)* represents the finite element mesh generated for the proposed 12/8 SRM model. The stator, rotor and air-gap regions are discretized into fine triangular elements to accurately capture magnetic field variations. A relatively dense mesh is applied in critical areas such as the air gap, teeth and flux barrier regions, ensuring better precision in flux density and torque calculations. The outer region uses a coarser mesh to reduce computational load while maintaining numerical stability. The proposed 12/8 SRM is initialized with 2D mesh and the maximum element size is given a 1mm to get the hysteresis, eddy current, copper and total losses of 6.957W, 0.280W ,307.426W and 196.35W respectively.

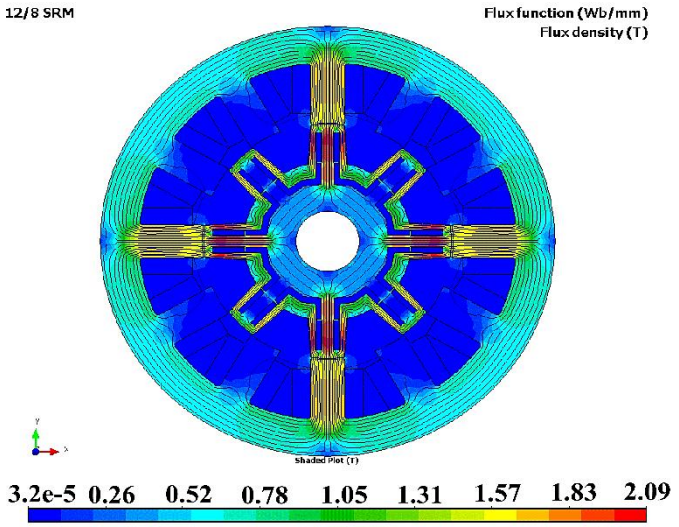

Figure 8(c). Flux distribution of proposed 12/8 SRM at 2.09T

The *figure 8(c)* infers the magnetic flux distribution in the 12/8 SRM with flux barriers under phase excitation. The energized stator poles attract the corresponding rotor poles, causing a strong flux concentration in those regions, which is shown in red and yellow colors. The flux flows through the rotor core and returns through the stator back iron, forming a closed loop. The blue regions indicate areas with low flux, mainly in the non-excited poles. The presence of flux barriers redirects the magnetic path, reducing leakage and improving the effective flux linkage required for torque production.

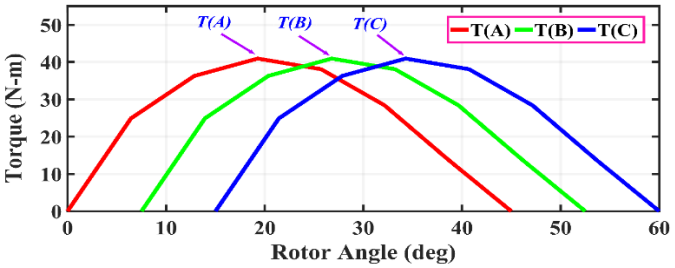

Figure 8(d). Torque characteristics of proposed 3 phase 12/8 SRM

The *figure 8(d)* infers the torque waveform produced by the Switched reluctance Motor of 6 stator poles and 2 rotor poles having the toque values of maximum, minimum, average,

FOREX Publication
Open Access | Rapid and quality publishing
International Journal of Electrical and Electronics Research (IJEER)
Research Article | Volume 13, Issue 4 | Pages 886-899 | e-ISSN: 2347-470X

Specific Torque density and Power Density vales of are 40.8 Nm, 38.9 Nm and 39.45 Nm, 17.85Nm/Kg and 1357.46W/Kg with torque ripple as 0.047.

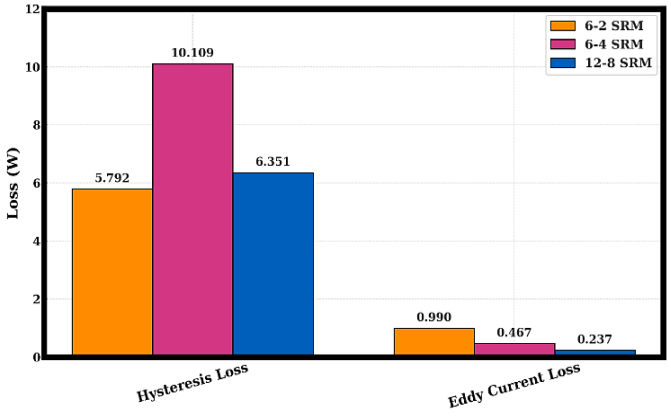

Figure 9(a). Hysteresis and Eddy current losses of 6/2,6/4 & 12/8 base SRM

The *figure 9(a)* compares hysteresis and eddy current losses for 6/2, 6/4 and 12/8 SRM configurations. The 6/4 SRM exhibits the highest hysteresis loss of 10.109 W, followed by the 12/8 SRM at 6.351 W and the 6/2 SRM at 5.792 W. In contrast, the eddy current loss is lowest in the 12/8 SRM at 0.237 W, while the 6/2 SRM records the highest value of 0.990 W. The results show that the 12/8 SRM offers a balanced reduction in both magnetic losses, making it superior to the other two machines in terms of core loss performance.

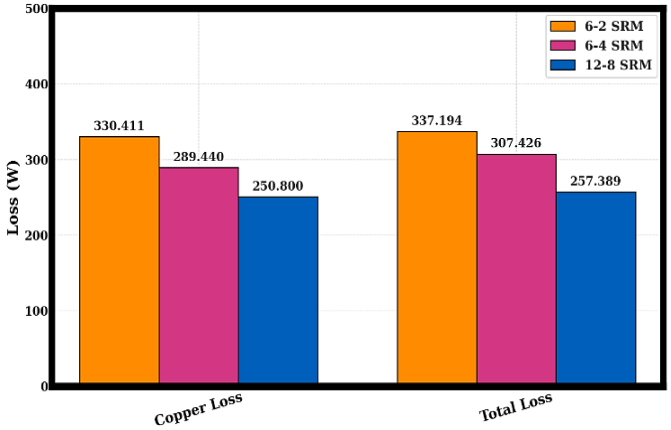

Figure 9(b). Copper and Total losses of 6/2,6/4 & 12/8 base SRM

The *figure 9(b)* infers the copper loss reduces as the stator and rotor poles increase. The highest copper loss is observed to be in the 6/2 SRM (330.411 W) then 6/4 SRM (289.440 W) the lowest copper loss is in the 12/8 SRM (250.800 W). The same pattern can be observed in the total loss spread, with the 12/8 SRM registering 257.389 W, 307.426 W and 337.194 W of the 6/4 SRM and 6/2 SRM. These comparisons infer the 12/8 SRM is the most efficient in its application of energy, due to its reduced electrical and magnetic losses.

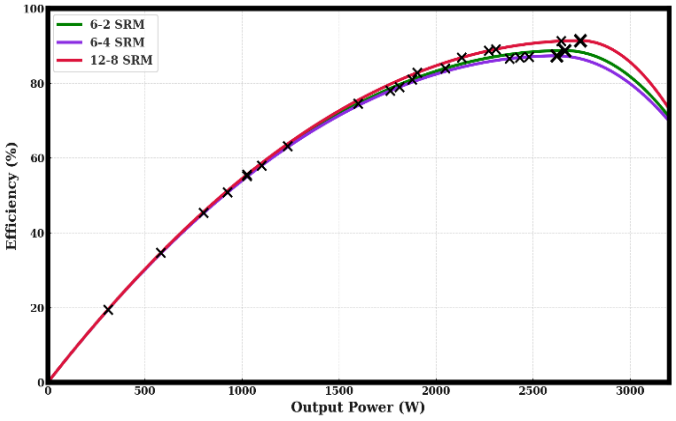

Figure 9(c). Efficiency curves of 6/2,6/4 & 12/8 base SRM

The *figure 9(c)* shows the efficiency curves of the 6/2, 6/4 and 12/8 base SRM designs. Within these topologies, the highest efficiency of the 12/8 SRM is observed in most operating points ranging just above 90 percent at the highest efficiency with 6/4 and 6/2 SRMs having slightly less maximum efficiencies. Beyond the optimum region, there follows a small loss of efficiency, which can be ascribed to an increase of conduction and switching losses. In general, the 12/8 SRM is the best in terms of efficiency performance within the entire operating range. Therefore, the relative evaluation of the losses and efficiency show that the 12/8 base SRM is the better design with a lower core and copper losses and high sustainability of high efficiency thus making it a better choice in the high-performance application.

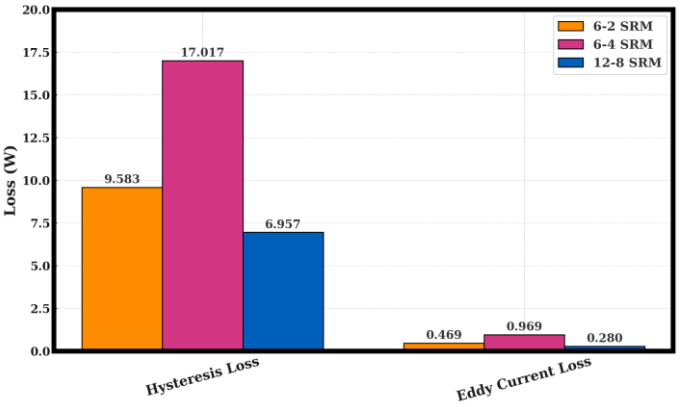

Figure 10(a). Hysteresis and Eddy current losses of 6/2, 6/4 & 12/8 Proposed SRM

The *figure 10(a)* shows the relative magnetic loss properties of three topologies of the synchronous reluctance motor (SRM). The hysteresis loss of the 6/4 SRM is the highest, and is 17.017 W, the 6/2 and 12/8 SRMs register loss values of 9.583 W and 6.957 W respectively. Concerning the eddy current losses, 12/8 SRM has the least loss of 0.280W compared to 0.469W in 6/2 SRM and 0.969W in 6/4 SRM. These results indicate that the 12/8 SRM exhibits the lowest overall magnetic loss, making it more efficient in core energy conversion.

FOREX Publication
Open Access | Rapid and quality publishing
International Journal of Electrical and Electronics Research (IJEER)
Research Article | Volume 13, Issue 4 | Pages 886-899 | e-ISSN: 2347-470X

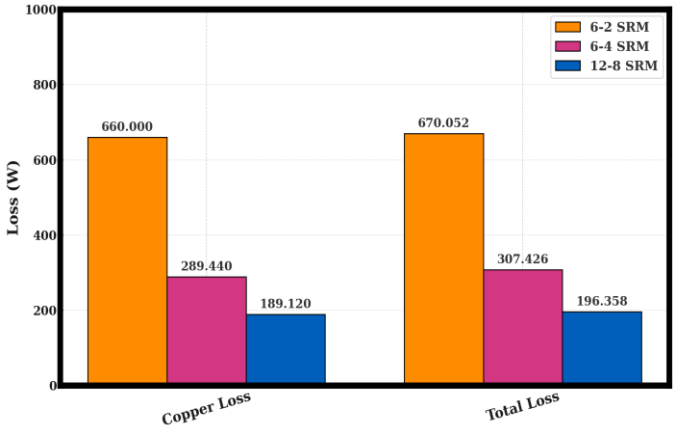

Figure 10(b). Copper and Total losses of 6/2,6/4 & 12/8 Proposed SRM

The *figure10(b)* infers the 6/2 SRM shows a high copper loss of 660 W, mainly due to fewer stator poles carrying more current per phase. The 6/4 SRM reduces this to 289.440 W, while the 12/8 SRM achieves the minimum value of 189.120 W. A similar pattern is identified in the total losses, where the 12/8 SRM records 196.358 W, much lower than the 307.426 W for 6/4 and 670.052 W for 6/2 SRM. Therefore, the 12/8 SRM provides the most optimized loss profile among the compared machines.

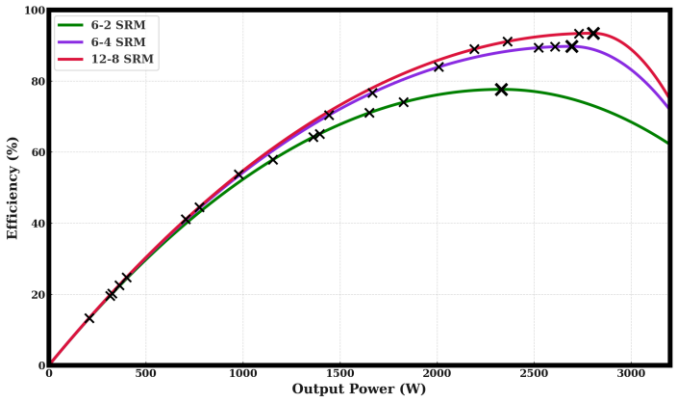

Figure 10 (c). Efficiency curves of 6/2,6/4 & 12/8 Proposed SRM

The *figure 10(c)* shows the efficiency curves of all three 6/2,6/4 & 12/8 Proposed SRM motors which improves the performance with increasing output power, reaching peak efficiency in the rated region. The 12/8 SRM consistently achieves the highest efficiency, nearing values above 90% around 2500 W, whereas the 6/4 SRM follows closely and the 6/2 SRM shows a noticeable drop beyond 2000 W due to increased resistive losses. Thus, the 12/8 SRM maintains superior efficiency across the entire operating range. Considering magnetic loss, copper loss and efficiency the 12/8 SRM is the best-performing configuration, making it highly suitable for high torque and high efficiency applications.

4. COMPARISION OF TORQUE AND LOSSES ANALYSIS

Table 1. Torque Characteristics in Base SRM Configurations

S. No	Base SRM Configuration	T_{min} (Nm)	T_{max} (Nm)	T_{avg} (Nm)	T_{ripple} (No Unit)	Mass of the motor (Kg)	Specific Torque Density (Nm /Kg)	Power Density W/Kg
1	**6/2**	17.7	18.5	18.1	0.044	2.01	9.00	1492.53
2	**6/4**	15.6	17.5	16.55	0.114	2.28	7.25	1315.78
3	**12/8**	19.8	25.9	22.85	0.266	2.81	8.13	1067.61

Table 2. Losses & Efficiency in Base SRM Configurations

S. No	Base SRM Configuration	Hysteresis Loss (W)	Eddy Current Loss (W)	Copper Loss (W)	Total Loss (W)	Input Power (W)	Output Power (W)	% Efficiency
1	**6/2**	5.792	0.990	330.411	337.194	3000	2662.806	88.7602
2	**6/4**	10.109	0.467	368.700	379.276	3000	2620.724	87.3575
3	**12/8**	6.351	0.237	250.800	257.389	3000	2742.611	91.42038

Table 3. Torque Characteristics in Proposed Single layer flux barrier SRM Configurations

S. No	Proposed SRM with single layer Flux barrier	Tmin (Nm)	Tmax (Nm)	Tavg (Nm)	Tripple (No Unit)	Mass of the motor (Kg)	Specific Torque Density (Nm/Kg)	Power Density (W/Kg)
1	**6/2**	20.9	30.5	25.7	0.37	2.12	12.12	1415.09
2	**6/4**	29.3	33.1	31.2	0.121	2.19	14.24	1369.86
3	**12/8**	38.9	40.8	39.45	0.047	2.21	17.85	1357.46

FOREX Publication
Open Access | Rapid and quality publishing
International Journal of Electrical and Electronics Research (IJEER)
Research Article | Volume 13, Issue 4 | Pages 886-899 | e-ISSN: 2347-470X

Table 4. Losses & Efficiency in Proposed Single layer flux barrier SRM Configurations

S. No	Proposed SRM with single layer Flux barrier	Hysteresis Loss (W)	Eddy Current Loss (W)	Copper Loss (W)	Total Loss (W)	Input Power (W)	Output Power (W)	% Efficiency
1	**6/2**	9.583	0.469	660.000	670.052	3000	2329.948	77.66494
2	**6/4**	17.017	0.969	289.440	307.426	3000	2329.948	89.7525
3	**12/8**	6.957	0.280	307.426	196.358	3000	2803.642	93.4547

The torque performance of the conventional Switched Reluctance Motor (SRM) configurations in *table1* infers that the 12/8 structure produces the highest average torque (22.85 Nm) due to increased rotor and stator pole interaction. Nevertheless, the torque ripple has a notable value of 0.266 which indicates electromagnetic vibrations to be very strong. The torque density quantifications measurements are in line with the hypothesis that the 6/2 rotor layout results in the best torque per unit mass ratio, while the 6/4 structure yields a lower one, and the 12/8 gives a trade-off with a higher torque magnitude. The 6/2 configuration shows a lower mean torque but at the same time has a lower torque ripple which means a better operational profile though at the cost of torque capacity.

Table 2 shows that the base SRM show large copper losses which means that there was considerable resistive heating of the stator windings. Compared to the 6 /4 design, the 6 /2 design is relatively low in magnetic losses which makes it to perform moderately with 88.76 %. Although 12/8 design is higher in torque potential, the peak efficiency of 91.42% assertion is high which refers to the higher use and the loss distribution is less.

The flux-barrier proposed structure is very efficient to the ability of the torque of all configurations discussed in *table 3*. The barriers increase anisotropy between the aligned and unaligned states, which increases a better change of the magnetic reluctance that is equal to the increase of more torques. The high topology of 12/8 gives a mean torque of 39.45 Nm and specific torque density of 17.85 Nm/ kg, in comparison, it has a huge performance enhancement over its base counterpart. In addition, the 6/2 and 12/8 designs are far superior in eliminating torque ripple and lead to a less discontinuous electro-magnetic torque response.

With the introduction of flux barriers, hysteresis and eddy current losses slightly increase in certain configurations due to localized flux concentration in the laminated core. However, the reduced copper losses in 6/4 and 12/8 structures indicate improved winding utilization and lower resistive stress. In the *table 4* 12/8 proposed model again shows superior performance with a maximum efficiency of 93.45%, proving that flux barriers effectively minimize energy dissipation while enabling higher output power.

5. THERMAL ANALYSIS OF 12/8 PROPOSED SINGLE LAYERED FLUX BARRIER OF SRM

The thermal performance assessment of the single layered flux barrier Switched Reluctance Motor (SRM) was carried out under rated electromagnetic loading to evaluate the transient state temperature distribution and hot spot formation within the machine structure. The heat generated mainly in the stator windings due to copper losses and in the rotor core due to core losses is transferring through conduction toward the stator yoke and motor housing. Air gap convection and external surface radiation further contributed to cooling behavior. The flux barrier arrangement played a significant role in improving thermal dissipation by reducing local saturation and minimizing iron loss concentration along the rotor path.

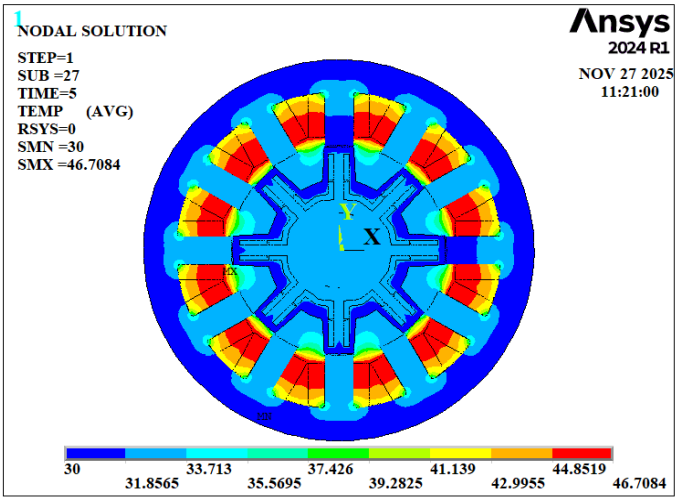

Figure 11. Thermal distribution of 12/8 Proposed SRM

The *figure 11* show a gradual increase in temperature with operating time and the machine reaches a near-steady thermal equilibrium after continuous operation. Temperature was highest at the stator winding section where the heat is best stored since conduction paths are few. The maximum temperature stabilized at some 46.7°C after about 5 hours of constant operation, which is also within the safe thermal limit of insulation Class B materials. This is to affirm that the proposed flux-barrier structure is effective in limiting thermal stress so that

FOREX Publication
Open Access | Rapid and quality publishing
International Journal of Electrical and Electronics Research (IJEER)
Research Article | Volume 13, Issue 4 | Pages 886-899 | e-ISSN: 2347-470X

there would be enhanced operational reliability and extended life span. All in all, the analysis confirms that the designed SRM is able to last long before it reaches the limits of acceptable thermal limits.

6. EXPERIMENTAL SETUP OF 12/8 PROPOSED SRM

The experimental hardware platform solution is designed in order to verify the functionality of the proposed 12/8 Switched Reluctance Motor (SRM) under realistic operating conditions as depicted in *figure 12*. The system is mainly composed of power conversion stage, control and gating circuitry, measurement instrumentation and the SRM drive. To provide the right isolation and voltage regulation, a step-down transformer is used at the input stage to feed the power electronic converter. This transformer supplies the required AC level of voltage which is then rectified and fed through the converter unit to supply the DC excitation required by motor phases.

The converter circuit has been designed and is including fast switching MOSFETs and freewheeling diodes to excite the various stator phases separately. The converter provides regulated current to the windings of the motor to produce the desired phase excitation sequence that is needed to produce torque. A special triggering circuit provides adequately synchronized gate pulses, which are based on a rotor position feedback system. The position feedback makes sure that it can do accurate commutation and reduce the torque ripple during the real time work.

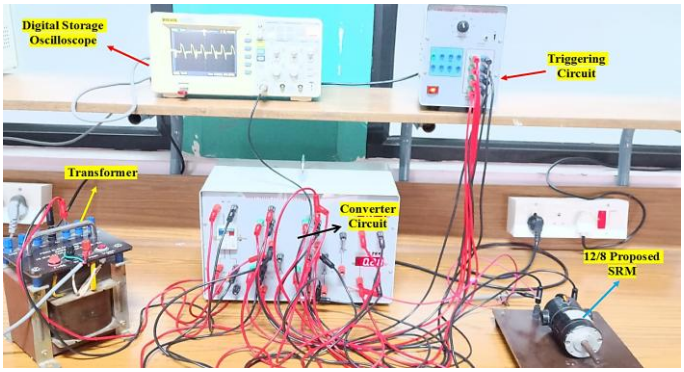

Figure 12. Experimental setup of 12/8 proposed SRM

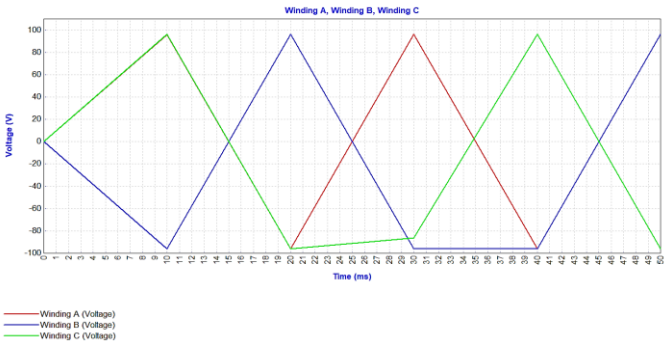

Figure 13. Excitation voltages of 12/8 proposed SRM

Figure 14. Phase voltage waveform of 12/8 proposed SRM

The voltage waveform of an experiment with the proposed 12/8 Switched Reluctance Motor (SRM) with a single-layered flux-barrier rotor is indicated in *figure 13* and *figure 14*. A Digital Storage Oscilloscope (DSO) is used to record the waveforms during dynamic excitation of the motor with bridge converter. The voltage pattern distinctly shows the typical switching nature of SRM drives; each pulse is the excitation and demagnetization of a single phase depending on the alignment of the rotor pole.

A sudden increase in voltage at the switching moment signifies the formation of phase energization in order to form magnetic flux in the aligned area of the flux-barrier rotor. The negative spike that came out uniquely every time the power converter was raised is an indication of effective demagnetization and recovery of the stored energy using the diodes of the power converter which act as freewheeling diodes. Small irregularities at high frequencies in the conduction interval are evident and these are related to switching transitions and parasitic inductances in the compact winding and flux barrier structural geometry.

The maximum measured phase voltage reaches approximately +12.8 V, whereas the negative recovery voltage dips to nearly –14.4 V, ensuring proper current decay before the next excitation interval. The periodicity of the waveform corresponds to the rotor slot-pole structure of the 12-stator/8-rotor configuration, supporting smooth torque generation with minimized magnetic saturation due to the flux-barrier design.

Table 5. Specifications of SRM

Parameters	Specifications
Supply voltage	96V
Air gap thickness	0.5mm
Coil fill Factor	60%
No of phases	3
No of Structures	6/2,6/4,12/8
Slot depth	21 mm
Stator Pole angle	15.5 deg
Rotor Pole angle	12 deg
Number of turns	110

FOREX Publication
Open Access | Rapid and quality publishing
International Journal of Electrical and Electronics Research (IJEER)
Research Article | Volume 13, Issue 4 | Pages 886-899|e-ISSN: 2347-470X

Coil Guage	Copper -24G
Core Material	M19-29Ga
Rated current	10 A
Rated speed	2700 rpm
Stack height	110 mm
Stator outer Diameter	150 mm
Shaft Diameter	20 mm
Meshing	1mm (Triangular type)

7. CONCLUSION

This study optimized various SRM rotor topologies to reduce torque ripple and enhance torque output for electric vehicle applications. Simulation has conducted using finite element analysis (FEA), considering multiple rotor configurations such as 6/2, 6/4, 12/8. These designs are selected based on flux distribution and mechanical integrity. Considering magnetic loss, copper loss and efficiency the 12/8 SRM is the best performing configuration, making it highly suitable for high torque and high efficiency applications. So, the 12/8 single layered flux barrier SRM configuration is the most suitable option for the proposed electric vehicle (EV) applications with an average torque of 39.45 Nm at an efficiency of 93.45%. Future work will explore with advanced materials to further minimize torque ripple and enhance efficiency.

Funding: This research received no external funding.

Conflicts of Interest: The authors declare no conflict of interest.

REFERENCES

[1] F. S. El-Faouri et al., "Torque Ripple Minimization in Switched Reluctance Motors with Acoustic Noise Mitigation by Current Waveform Shaping," in IEEE Open Journal of Industry Applications, vol. 6, 2025 pp. 403-414, doi: 10.1109/OJIA.2025.3579150.

[2] J. Sawant, D. Shahakar and P. Pandit, "Enhancing EV Performance: Critical Review of ITC and DTC for Torque Ripple Mitigation in SRMs," 2025 1st International Conference on AIML-Applications for Engineering & Technology (ICAET), Pune, India, pp.1-7, 2025, doi:10.1109/ICAET63349.2025.10 932198.

[3] X. Yao, H. He, J. Wang and Q. Guan, "An Online Torque Sharing Function Method for Low Torque Ripple and Copper Losses in Switched Reluctance Motors," 2024 IEEE 10th International Power Electronics and Motion Control Conference (IPEMC2024-ECCE Asia), Chengdu, China, 2024, pp. 1984-1989, doi: 10.1109/IPEMC-ECCEAsia60879.2024.10567956.

[4] Z. Li, S. Wang and L. Zhou, "An Online Torque Sharing Function with Torque Reference Self-Adjusting Method for Switched Reluctance Machines," 2024 27th International Conference on Electrical Machines and Systems (ICEMS), Fukuoka, Japan, 2024, pp. 598-603, doi: 10.23919/ICEMS60997.2024.10921356.

[5] T. Li, Z. Xu, Y. Zhang, D. -H. Lee and Y. Bao, "Characteristics Analysis of a Novel Permanent Magnet Assisted 12/8 Segmental Rotor Type Switched Reluctance Motor," 2024 27th International Conference on Electrical Machines and Systems (ICEMS), Fukuoka, Japan, 2024, pp. 762-767, doi: 10.23919/ICEMS60997.2024.10921312.

[6] S. K. Chaurasiya, A. Bhattacharya and S. Das, "Development of a 6/4 Switched Reluctance Motor for Torque Improvement in Solar Water Pumping System," 2024 International Conference on Electrical Machines (ICEM), Torino, Italy, 2024, pp. 1-7, doi: 10.1109/ICEM60801.2024.10700533.

[7] Y. Tecklehaimanot, M. Elgendy, S. Odhano and V. Pickert, "Reducing Torque Ripple in Switched Reluctance Motors Using a Novel Power Converter," IECON 2024 - 50th Annual Conference of the IEEE Industrial Electronics Society, Chicago, IL, USA, 2024, pp.1-6, doi:10.1109/IECON55916.2024 .10905152.

[8] J. Parmar, J. Panchal, T. Jhankal and A. N. Patel, "Selection of Stator Pole Tip for Torque Ripple Reduction of Switched Reluctance Motor," *2024 IEEE 11th Power India International Conference (PIICON)*, JAIPUR, India, 2024, pp. 1-6, doi: 10.1109/PIICON63519.2024.10995057.

[9] I. Shimohama, K. Ohyama, H. Fujii, H. Uehara and Y. Hyakutake, "Static Torque Characteristics of SRM with a Three-Dimensional Gap Structure," 2024 27th International Conference on Electrical Machines and Systems (ICEMS), Fukuoka, Japan, 2024, pp. 1879-1883, doi: 10.23919/ICEMS60997.2024.10921367.

[10] G. Rizzoli, L. Vancini, M. Mengoni, G. Sala, L. Zarri and A. Tani, "Torque and Current Ripple Analysis in Integrated DC-DC Boost Chargers Based on SynRMs and WR-SMs," 2024 International Conference on Electrical Machines (ICEM), Torino, Italy, 2024, pp. 1-8, doi: 10.1109/ICEM60801.2024.10700311.

[11] R. Asati, D. S. Bankar and A. L. Nehete, "Torque Ripple Assessment of Converter Topologies for Switched Reluctance Motor," 2024 IEEE 3rd International Conference on Electrical Power and Energy Systems (ICEPES), Bhopal, India, 2024, pp. 1-6, doi: 10.1109/ICEPES60647.2024.10653612.

[12] V. Abhijith, M. J. Hossain, G. Lei, P. A. Sreelekha and S. B. Kadam, "High Torque Capability Non-Permanent Magnet Hybrid Excited Switched Reluctance Motor for Electric Vehicle Application," 2023 IEEE Energy Conversion Congress and Exposition (ECCE), Nashville, TN, USA, 2023, pp. 3851-3858, doi: 10.1109/ECCE53617.2023.10362416.

[13] P. R, V. R and C. R. Balamurugan, "Rotor Design and Modeling for Switched Reluctance Motor to Minimize Torque Ripples," 2023 International Conference on System, Computation, Automation and Networking (ICSCAN), PUDUCHERRY, India,2023, pp.1-5, doi:10.1109/ICSCAN58655.202 3.10395436.

[14] V. Abhijith, M. J. Hossain, G. Lei, P. A. Sreelekha and S. B. Kadam, "Hybrid Topologies of Non-Permanent Magnet-Excited Switched-Reluctance Motors with High Torque Capability for Electric Vehicle Applications," 2023 IEEE International Future Energy Electronics Conference (IFEEC), Sydney, Australia, 2023, pp. 120-124, doi: 10.1109/IFEEC58486.2023.10458487.

[15] C. E. Abunike, O. I. Okoro, I. E. Davidson, U. B. Akuru and A. S. Sumeet, "Torque Ripple Reduction of Switched Reluctance Motor Topologies Parameterized with FEM Data for Electromechanical Brake System," 2022 4th International Conference on Emerging Trends in Electrical, Electronic and Communications Engineering (ELECOM), Mauritius, 2022, pp. 1-6, doi:10.1109/ELECOM 54934.2022.9965232.